Supplementary Information

Tuning the crystal structure, optical band gap and persistent luminescence performance of Cr^{3+}-doped $LiGa_5O_8$ spinel by adding aluminum and indium

Anastasiia Karabut[a], Halyna Zhydachevska[a], Łukasz Wachnicki[a], Vasyl Hreb[b], Leonid Vasylechko[b,*], Yuriy Hizhnyi[c,d], Tetiana Shevtsova[c], Andriy Luchechko[e], Agnieszka Pieniążek[a], Marek Berkowski[a], Yaroslav Zhydachevskyy[a,*]

[a] Institute of Physics, Polish Academy of Sciences, aleja Lotników 32/46, Warsaw 02-668, Poland

[b] Lviv Polytechnic National University, S. Bandera Str. 12, Lviv 79013, Ukraine

[c] Donetsk Institute for Physics and Engineering of NAS of Ukraine, Kyiv 03028, Ukraine

[d] Taras Shevchenko National University of Kyiv, Volodymyrska Str. 64/13 Kyiv 01601, Ukraine

[e] Ivan Franko National University of Lviv, Tarnavskogo Str. 107, Lviv 79017, Ukraine

Corresponding author: Email: zhydach@ifpan.edu.pl, leonid.o.vasylechko@lpnu.ua

This files includes:

Fig. S1. Graphical results of Rietveld refinement of the selected $LiGa_5O_8$-based spinel structures. Experimental XRD patterns (blue circles) are shown along with calculated profiles (red lines) and difference curves between them. Short vertical bars indicate the positions of Bragg's maxima in the cubic $P4_332$ spinel structure.

Fig. S2. Graphical results of Rietveld refinement of chromium doped $LaGa_5O_8$-based materials annealed in vacuum.

Fig. S3. Concentration evolution of the lattice parameters and the nearest cation-oxygen distances in the $Li(Ga_{1-x}M_x)_5O_8$ series.

Fig. S4. The 2×2×2 super-cell of $LiGa_5O_8$ crystal.

Table S1. Numbers of cationic substitutions modeled in 2x2x2 super-cells of $Li(Ga_{1-x-y}Al_xIn_y)_5O_8$.

Table S2. DFT-optimized lattice parameters of $Li(Ga_{1-x-y}Al_xIn_y)_5O_8$ alloys.

Fig. S5. Calculated low-energy parts of absorption spectra of $Li(Ga_{1-x-y}Al_xIn_y)_5O_8$ crystals.

Fig. S6. A comparison of the TSL curves of the studied samples (as-synthesized and annealed in a vacuum) registered at 718 nm after UV (270-310 nm) exposure at a liquid nitrogen temperature. Heating rate 1 C/s.

Fig. S7. The PLE spectra of the studied samples measured using synchrotron irradiation at room temperature (registered at 718 nm), and their deconvolution by Gaussian peaks.

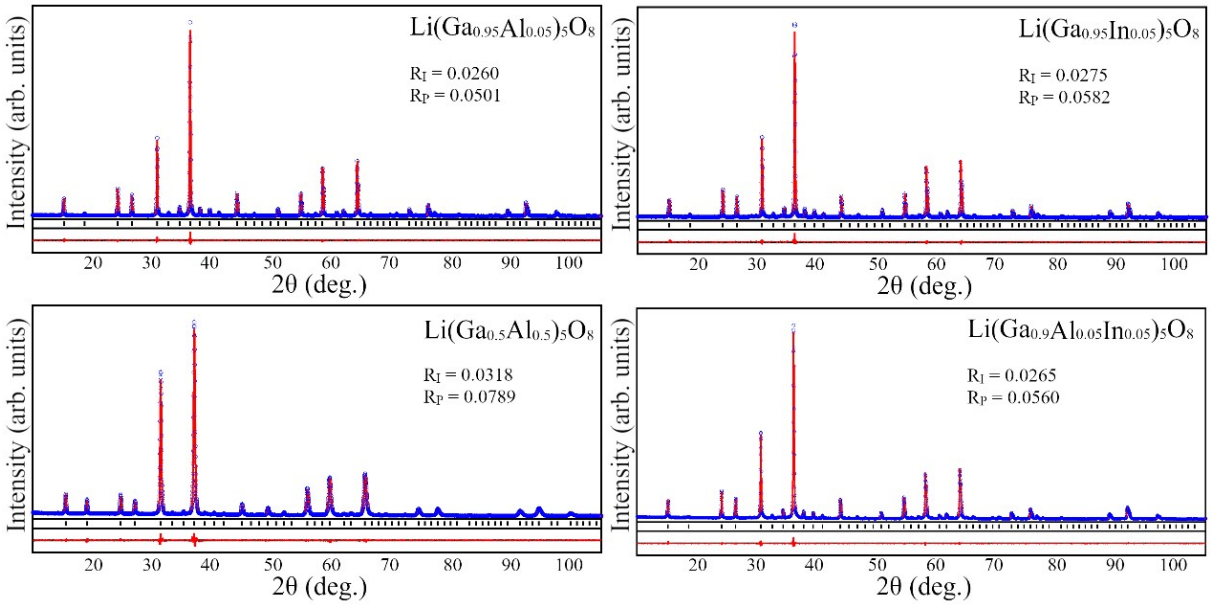

Fig. S1. Graphical results of Rietveld refinement of the selected $LiGa_5O_8$-based spinel structures. Experimental XRD patterns (blue circles) are shown along with calculated profiles (red lines) and difference curves between them. Short vertical bars indicate the positions of Bragg's maxima in the cubic $P4_332$ spinel structure.

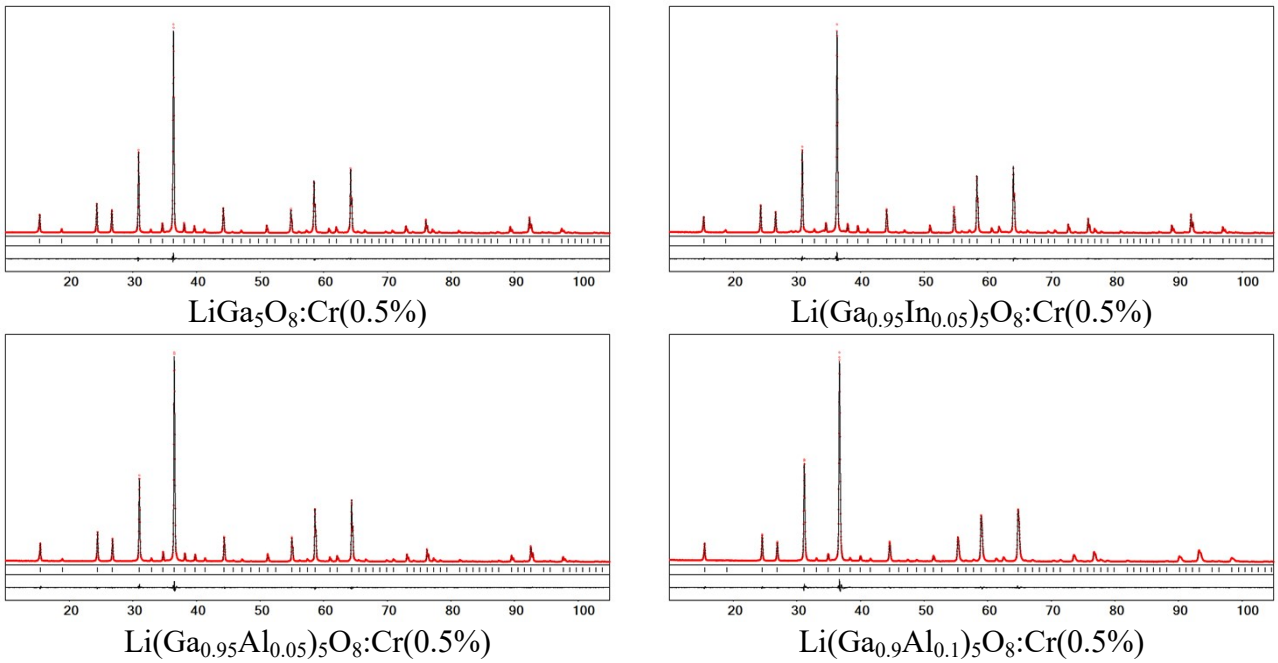

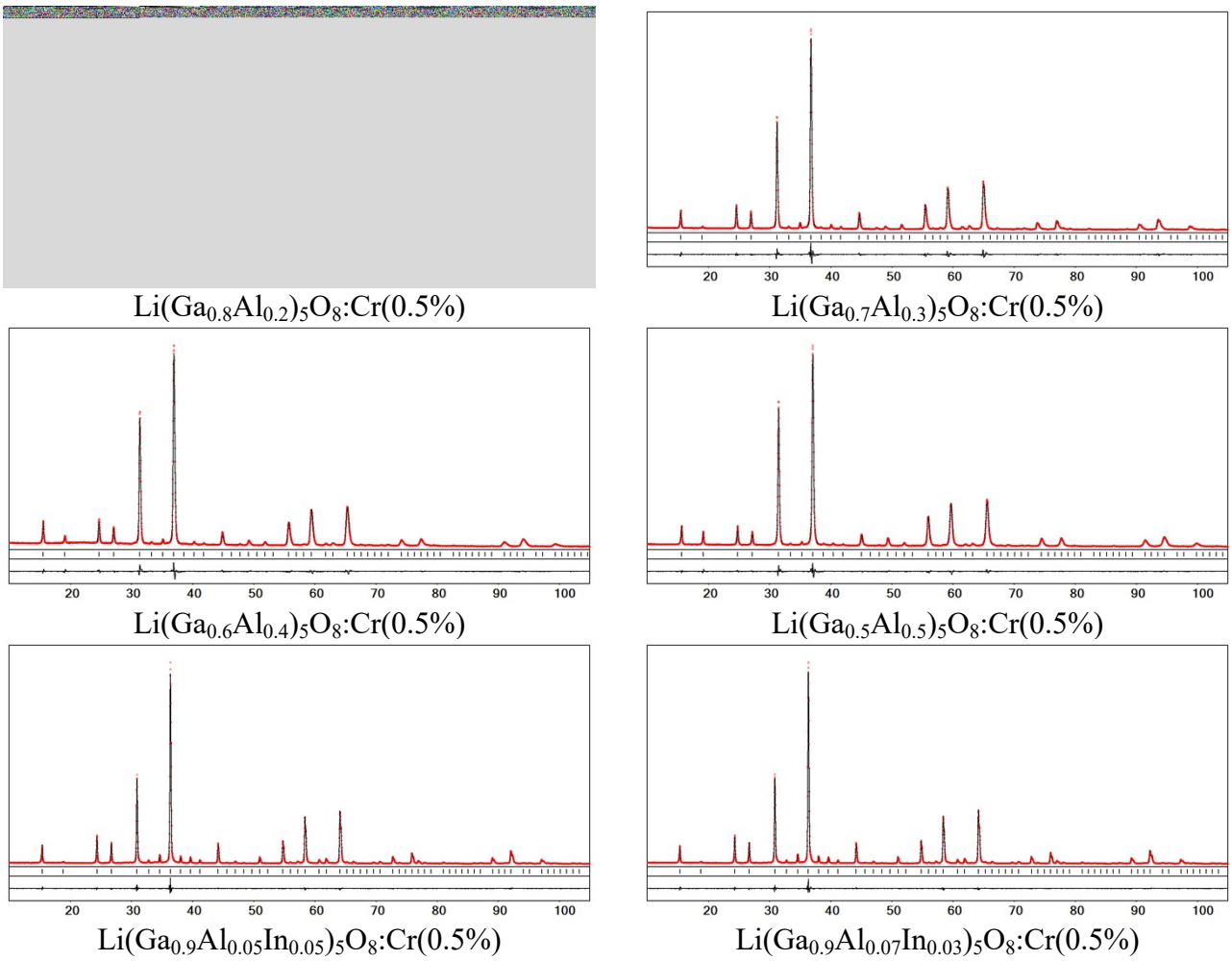

Fig. S2. Graphical results of Rietveld refinement of chromium doped $LaGa_5O_8$-based materials annealed in vacuum. Experimental (red dots) and calculated (black lines) XRD profiles and its difference curves (in the bottom of each panel) are shown for the corresponding materials.

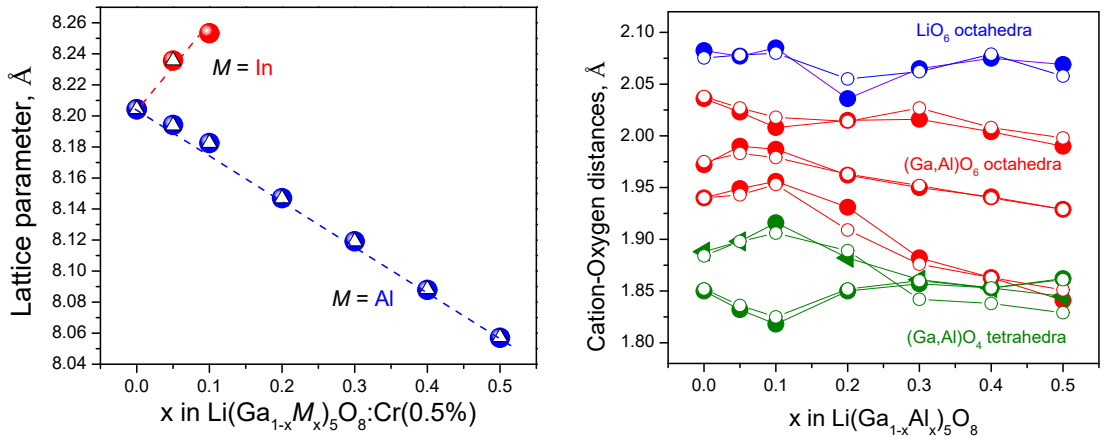

Fig. S3. Concentration evolution of the lattice parameters (left) and the nearest cation-oxygen distances (left) in the $Li(Ga_{1-x}M_x)_5O_8$ series. Solid and open symbols corresponds to the as-obtained in air samples and further vacuum annealed specimens, respectively.

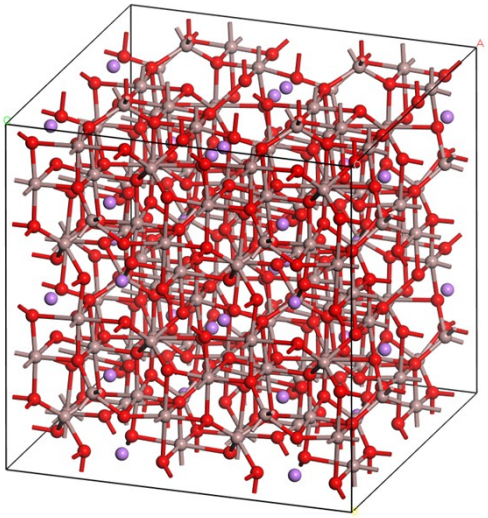

Fig. S4. The 2×2×2 super-cell of $LiGa_5O_8$ crystal.

Table S1. Numbers of cationic substitutions modeled in 2x2x2 super-cells of $Li(Ga_{1-x-y}Al_xIn_y)_5O_8$.

Chemical formula	Number of cations (Composition, %)		
	Ga	Al	In
$LiGa_5O_8$	160	0	0
$Li(Ga_{0.95}Al_{0.05})_5O_8$	152	8 (5)	0
$Li(Ga_{0.9}Al_{0.1})_5O_8$	144	16 (10)	0
$Li(Ga_{0.8}Al_{0.2})_5O_8$	128	32 (20)	0
$Li(Ga_{0.7}Al_{0.3})_5O_8$	112	48 (30)	0
$Li(Ga_{0.6}Al_{0.4})_5O_8$	96	64 (40)	0
$Li(Ga_{0.5}Al_{0.5})_5O_8$	80	80 (50)	0
$Li(Ga_{0.95}In_{0.05})_5O_8$	160	0	8 (5)
$Li(Ga_{0.9}In_{0.1})_5O_8$	152	0	16 (10)
$Li(Ga_{0.9}Al_{0.05}In_{0.05})_5O_8$	144	8 (5)	8 (5)
$Li(Ga_{0.9}Al_{0.07}In_{0.03})_5O_8$	144	11 (6.8)	5 (3.1)
$Li(Ga_{0.8}Al_{0.14}In_{0.06})_5O_8$	128	22 (13.8)	10 (6.3)

Table S2. DFT-optimized lattice parameters of $Li(Ga_{1-x-y}Al_xIn_y)_5O_8$ alloys.

Al-doped							
Lattice parameter	*x*						
	0	0.05	0.1	0.2	0.3	0.4	0.5
a ,Å	8.345	8.3261	8.30639	8.26942	8.23394	8.20348	8.16631
V, Å^3	1162.28413	1154.39854	1146.21563	1130.97998	1116.48437	1104.13869	1089.19971

In-doped, Al, In-codoped					
Lattice parameter	*y*		*x*, *y*		
	0.05	0.1	0.3 (*x* = 0.07, *y* = 0.03)	0.5 (*x* = 0.05, *y* = 0.05)	0.6 (*x* = 0.14, *y* = 0.06)
a ,Å	8.38544	8.42772	8.3448	8.36732	8.3458
V, Å^3	1179.25275	1197.18316	1162.19343	1171.62657	1162.6075

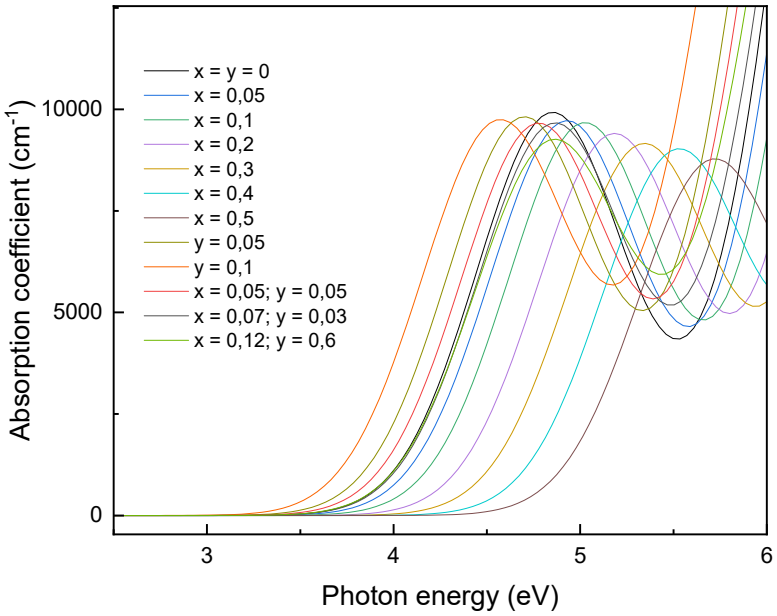

Fig. S5. Calculated low-energy parts of absorption spectra of $Li(Ga_{1-x-y}Al_xIn_y)_5O_8$ crystals.

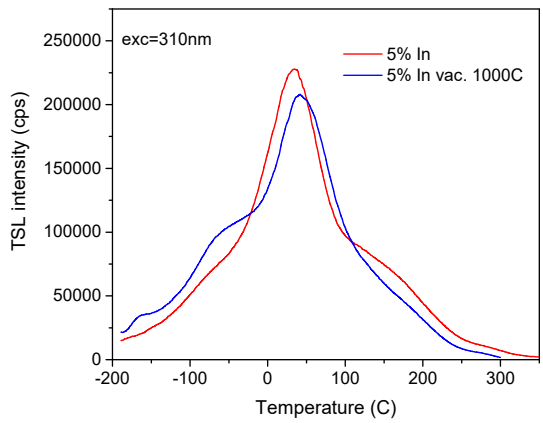
exc=310nm
5% In
5% In vac. 1000C
TSL intensity (cps)
Temperature (C)

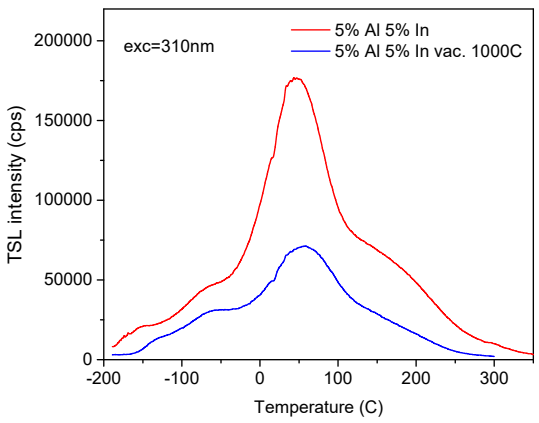
exc=310nm
5% Al 5% In
5% Al 5% In vac. 1000C
TSL intensity (cps)
Temperature (C)

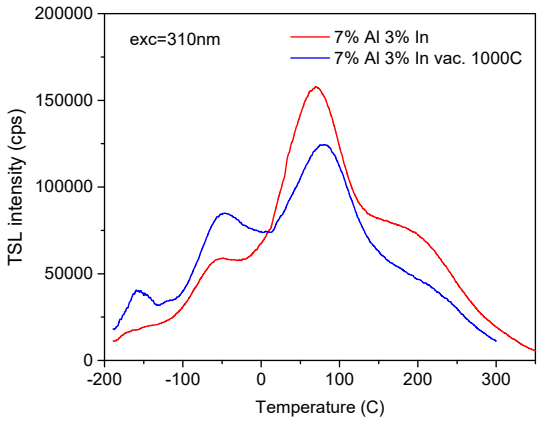
exc=310nm
7% Al 3% In
7% Al 3% In vac. 1000C
TSL intensity (cps)
Temperature (C)

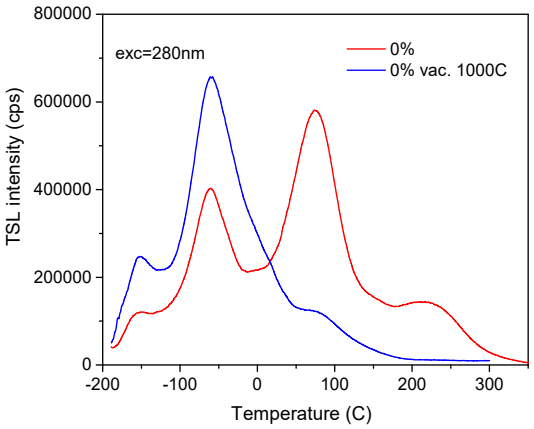
exc=280nm
0%
0% vac. 1000C
TSL intensity (cps)
Temperature (C)

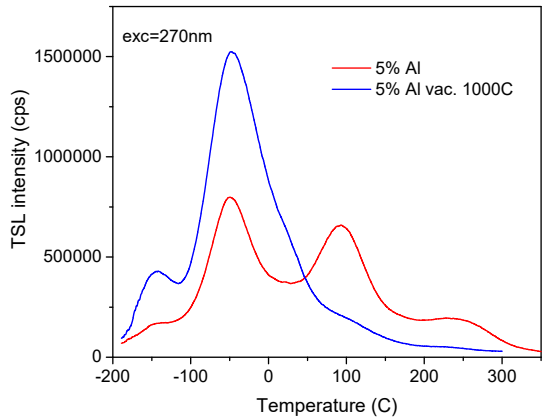
exc=270nm
5% Al
5% Al vac. 1000C
TSL intensity (cps)
Temperature (C)

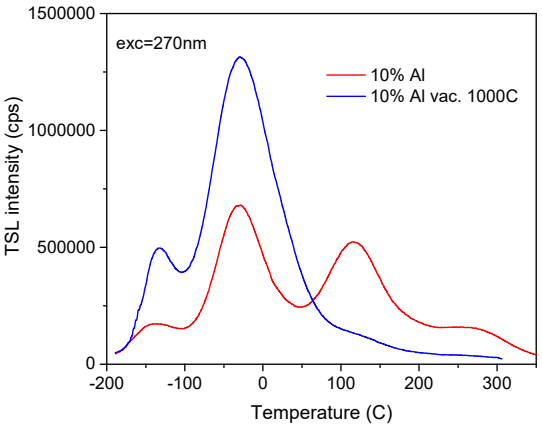
exc=270nm
10% Al
10% Al vac. 1000C
TSL intensity (cps)
Temperature (C)

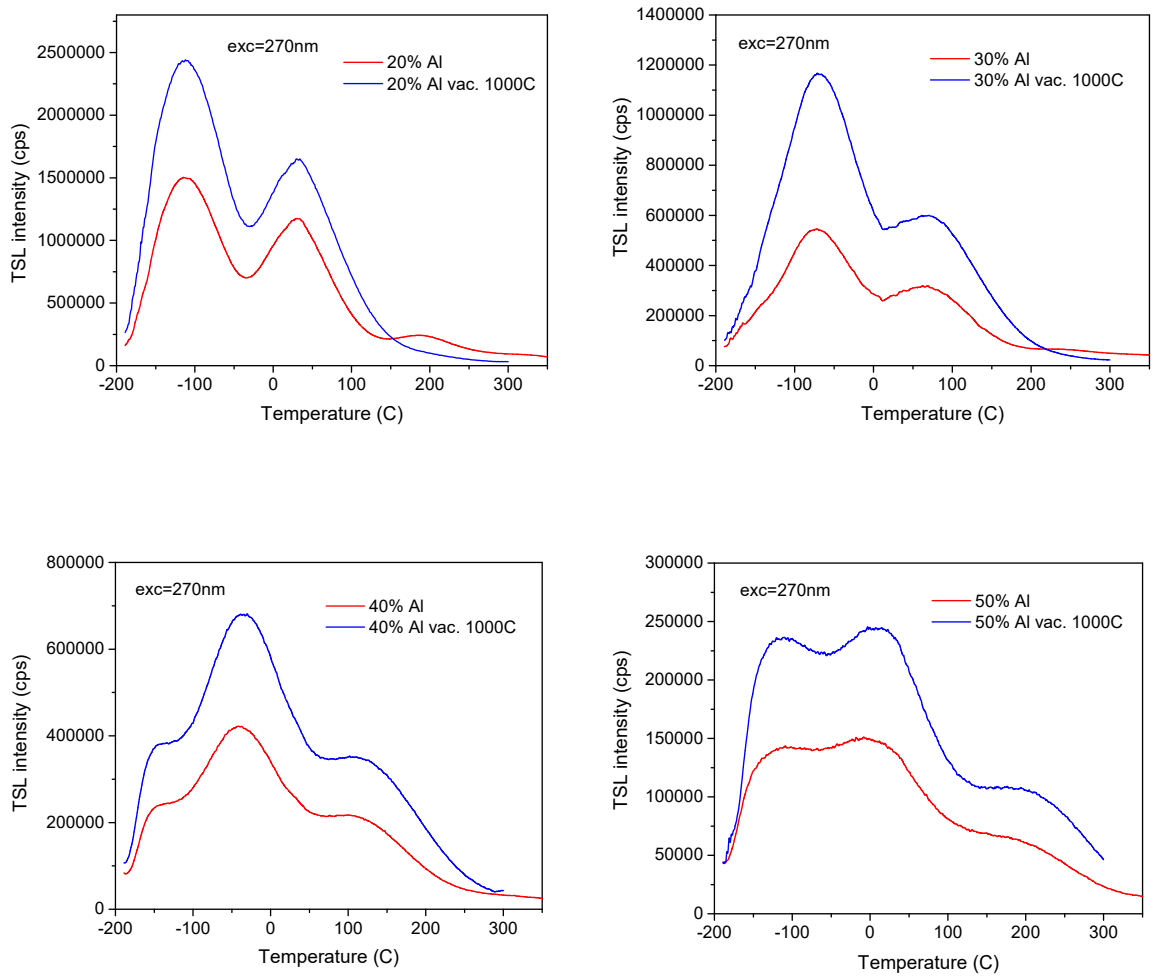

Fig. S6. A comparison of the TSL curves of the studied samples (as-synthesized and annealed in a vacuum) registered at 718 nm after UV (270-310 nm) exposure at a liquid nitrogen temperature. Heating rate 1 C/s.

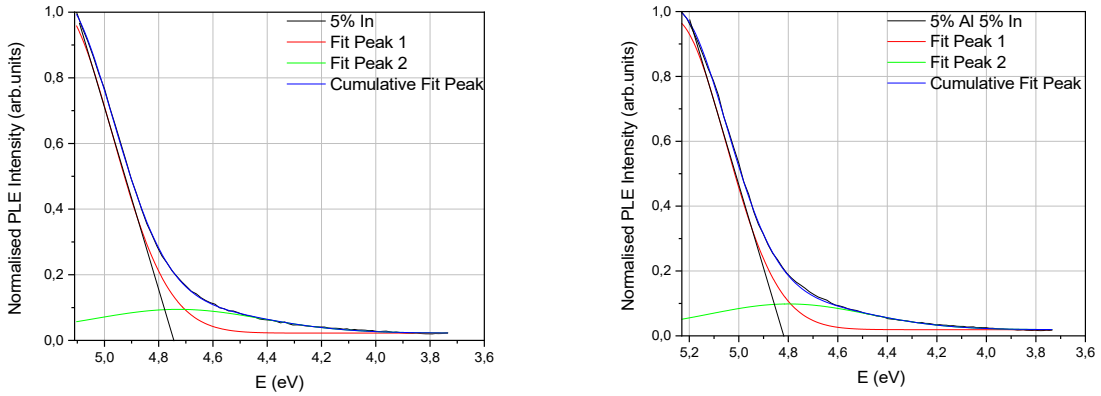

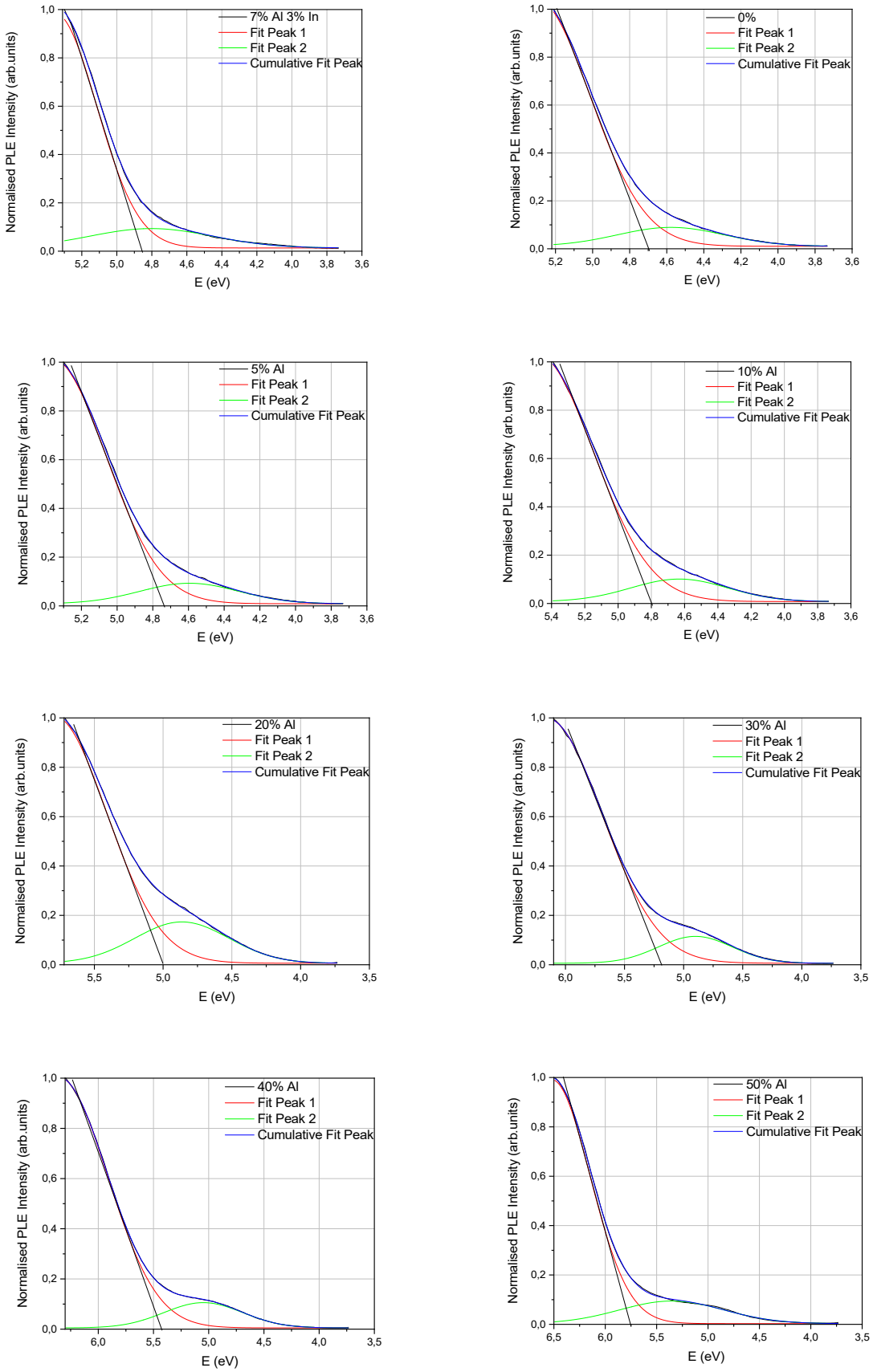

Fig. S7. The PLE spectra of the studied samples measured using synchrotron irradiation at room temperature (registered at 718 nm), and their deconvolution by Gaussian peaks.